Elucidating the Physical Property of the InGaN Nanorod Light-Emitting Diode: Large Tunneling Effect

Ya-Ju Lee, Chia-Jung Lee, Chih-Hao Chen, Tien-Chang Lu, *Member, IEEE*, and Hao-Chung Kuo, *Senior Member, IEEE*

***Abstract*—The current–voltage (I–V) characteristics of the InGaN nanorod light-emitting diode (LED) are evaluated using nanoprobes installed on a field-emission scanning electron microscope. The saturated current of the InGaN nanorod LED ($I_O = 2 \times 10^{-9}$ A) is found to be orders of magnitude higher than those obtained by downscaling a conventional InGaN LED to a chip size of 300×300 μm^2 ($I_{O1} = 1 \times 10^{-25}$ A; $I_{O2} = 1 \times 10^{-14}$ A). This observation is explained by the fact that the nanorod LED is associated with enhanced tunneling of injected carriers and, therefore, reduction of the defect-assisted leakage current and the diffusion–recombination process that normally occurs in InGaN LEDs.**

***Index Terms*—Light-emitting diode (LED), nanorod, tunneling effect.**

I. Introduction

SEMICONDUCTOR nanostructures are expected to be critical components of role in future optoelectronic devices [1], [2]. The possibility of quantum confinement [3], strain relaxation [4], and high crystallographic quality [5] make InGaN nanorods potential contenders for nanolaser [6], [7] and nano-LED [8]–[10], and provide a brand new approach for data storage, optical interconnects, and general lighting. Despite recent progress in nanofabrication techniques, a physical understanding of operating properties of nanodevices is still required to improve their performance and investigate their potential applications. In this paper, we will introduce the unique physical property observed in the nanorod LEDs. We investigate the current–voltage (I–V) characteristics of InGaN nanorod LEDs using nanoprobes installed on a field-emission scanning electron microscope (SEM). The saturation current ($I = 2 \times 10^{-9}$ A) and ideality factor ($n_{\mathrm{ideal}} = 25$) of the nanorod LED were much larger than those of a conventional LED with a chip size of 300×300 μm^2. The implications of the differences between the electrical characteristics of nanorod and conventional LEDs are discussed. The effect of enhanced tunneling on forward current is suggested to explain this anomalous electrical behavior in the nanorod LED.

Manuscript received June 28, 2010; revised July 20, 2010; accepted July 29, 2010. Date of publication September 20, 2010; date of current version August 5, 2011. This work was supported by the National Science Council of the Republic of China in Taiwan under Contract NSC-98-2112-M003-001-MY2.

Y.-J. Lee, C.-J. Lee, and C.-H. Chen are with the Institute of Electro-Optical Science and Technology, National Taiwan Normal University, Taipei 116, Taiwan (e-mail: yajulee@ntnu.edu.tw; maikuraki25@gmail.com; 697480308@ntnu.edu.tw).

T.-C. Lu and H.-C. Kuo are with the Department of Photonics and the Institute of Electro-Optical Engineering, National Chiao Tung University, Hsinchu 300, Taiwan (e-mail: timtclu@mail.nctu.edu.tw; hckuo@faculty.nctu.edu.tw).

Color versions of one or more of the figures in this paper are available online at http://ieeexplore.ieee.org.

Digital Object Identifier 10.1109/JSTQE.2010.2064287

II. Experiment

An LED wafer was grown on c-axis sapphire substrates by low-pressure metal-organic chemical-vapor deposition. Following the growth of a GaN nucleation layer at 520 °C, a 1.5-μm-thick undoped GaN buffer layer and a 2.5-μm-thick Si-doped n-type (5×10^{17} cm^{-3}) GaN cladding layer were grown at 1050 °C. The active region consisted of five periods of 2.5 nm $In_{0.23}Ga_{0.77}N$/10 nm GaN multiquantum wells (MQWs, $\lambda = 450$ nm) with Si doping in GaN barriers to reduce the quantum-confined stark effect. Finally, a 200-nm-thick Mg-doped p-type (3×10^{17} cm^{-3}) GaN cladding layer with a 50-nm-thick AlGaN electron-blocking layer was grown on the top at 1050 °C. To form nanorod arrays, a 5-nm-thick nickel (Ni) metal film was then deposited on the LED wafer by electron-beam evaporations. The sample underwent rapid thermal annealing at 850 °C for 60 s in ambient nitrogen to yield randomly distributed Ni metal islands with nanodimensions on the LED wafer surface, serving as a hard mask in the subsequent inductively coupled plasma (ICP) process. Then, 3 min of dry etching was conducted to ensure that the MQWs and n-type GaN nanorod arrays were exposed to the air. To form an ohmic contact, Ni nanodots were kept on the top of the nanorod arrays. Similarly, Ti/Al/Ti/Au layers were deposited and annealed at 600 °C to form ohmic contacts with an exposed n-type GaN layer.

The nanorod LED was then subjected to a Zyvex nanomanipulator system to determine the I–V characteristics. A conventional LED counterpart with a typical chip size of 300×300 μm^2 was also fabricated for comparison. Fig. 1(a) schematically depicts the nanoprobe setup, which includes nanorod LED arrays, a nanotip, an n-electrode pad (Ti/Al/Ti/Au), and Ni nanodots. Therefore, the nanotip with an internal diameter of 50 nm in the SEM enabled a p-contact to be made directly on the top of the nanorods, while another tip was located at the n-electrode, serving as the second contact, as displayed in Fig. 1(b). This setup was, therefore, able to measure the I–V characteristics of an individual nanorod. Fig. 1(c) presents an SEM image of a nanotip that is touching the top surface of a single nanorod. In this figure, the scale bar represents 100 nm. In this investigation, the mean diameters and the lengths of the nanorods are 80–100 and 350 nm, respectively. The general morphology and exterior

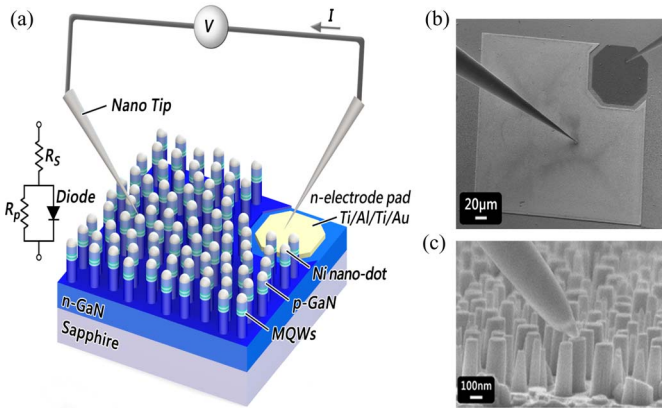

Fig. 1. (a) Probing test of a single nanorod LED performed using nanoprobes installed on the field-emission SEM. (Inset) Effective electrical circuit of the nanorod LED. (b) Electrical connection to a nanorod via two nanotips on the field-emission SEM. (c) Representative SEM image of nanotip in contact with the top of nanorod.

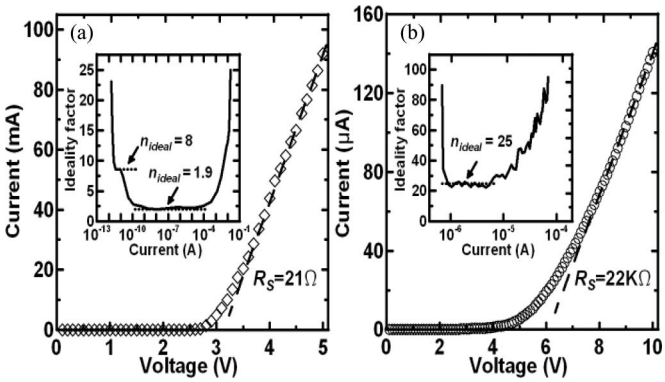

Fig. 2. I–V curves on linear-scale for (a) conventional and (b) single nanorod LEDs. Insets: Ideality factors against injected currents of conventional and single nanorod LEDs.

appearance of the nanorods in the SEM images are strongly determined by the annealing conditions of the Ni film and the ICP etching process [11]. The inset in Fig. 1(a) also presents the effective electrical circuit of an LED, where R_S and R_P represent the series and parallel resistances, respectively. Generally, R_S is determined by excessive contact resistance or by the resistance of the neutral regions, and R_P can be caused mainly by damage to junction regions during the ICP process or by surface imperfections. These parasitic resistances in the nanorod were taken into account in the subsequent calculation.

III. Results and Discussion

Fig. 2 plots the forward-bias I–V curves on a linear scale for (a) conventional and (b) single nanorod LEDs, respectively. These I–V characteristics were collected and averaged from ten conventional and nanorod LEDs. The R_S values, determined from these figures, are 21 Ω and 22 kΩ for conventional and single nanorod LEDs, respectively.

R_S in the single nanorod LED is orders of magnitude higher than in the conventional LED primarily because of the small feature size and the high contact resistance of the contact between the nanotip and the nanorod, resulting in a higher turn–on voltage for the single nanorod (∼6.1 V) than of the conventional LED (∼3.2 V). The insets in Fig. 2 display the ideality factors (n_{ideal}) of both LED samples obtained from the measurements using $n_{\text{ideal}} = (q/kT)((\partial \ln I/\partial V)^{-1})$ [12]. Clearly, in the inset in Fig. 2(a), the two distinct ideality factors $n_{\text{ideal}} = 8.0$ (3.7×10^{-12} A $< I < 1 \times 10^{-11}$ A) and $n_{\text{ideal}} = 1.9$ (8.0×10^{-10} A $< I < 5.0 \times 10^{-5}$ A) were determined for the conventional LED. Cao *et al.* found that in the InGaN-based LED, carrier recombination in the depletion region via dislocation defects, and therefore, leakage currents associated with deep-level traps, causes the ideality factor to exceed 2.0 [13]. In addition, increasing the forward bias causes the defect-assisted leakage current to reach its maximum and then saturate. Consequently, the diffusion–recombination current begins to flow through the depletion region and dominate the LED, yielding an ideality factor of between 1.0 and 2.0. Basically, the conventional LED acts as described. However, the I–V characteristic of the nanorod LED reveals completely different rectification behavior. For a single nanorod LED, a single value of the ideality factor $n_{\text{ideal}} = 25.0$ (9.0×10^{-7} A $< I < 5.5 \times 10^{-6}$ A) can be derived, as presented in the inset in Fig. 2(b). Importantly, such a large ideality factor is not likely to be attributable to the defect-assisted leakage current because the dislocation defect is barely detected for the nanorod LED with a diameter less than 100 nm, suggesting that in the nanorod LED, mechanisms of carrier recombination other than the defect-assisted leakage mechanism apply.

To analyze further the I–V properties of the conventional LED, the Shockley equation was modified to take into account the diffusion–recombination and defect-assisted leakage currents, as well as the parasitic effect, which is shown in the diode-circuit model in the inset in Fig. 1(a) [14]. Accordingly, the total injected current of LEDs I is given by

$$I = I_P + I_J = I_P + I_{\text{diffusion}} + I_{\text{leakage}} \tag{1}$$

where I_P represents the current that bypasses the junction region and is given by $I_P = (V - IR_S)/R_P$, I_J is the current that flows across the junction, and comprises the diffusion–recombination current $I_{\text{diffusion}}$ and the defect-assisted leakage current I_{leakage}. Both $I_{\text{diffusion}}$ and I_{leakage} are given by

$$I_{\text{diffusion}} = I_{O1}\left(\exp\left(\frac{e(V - IR_S)}{n_1 kT}\right) - 1\right) \tag{2}$$

$$I_{\text{leakage}} = I_{O2}\left(\exp\left(\frac{e(V - IR_S)}{n_2 kT}\right) - 1\right) \tag{3}$$

where I_{O1} and I_{O2} are saturation currents produced by the diffusion–recombination and the defect-assisted leakage processes, respectively, and n_1 and n_2 are the ideality factors for the diffusion–recombination and the defect-assisted leakage processes, respectively. Substituting (2) and (3) into (1) and considering $I_P = (V - IR_S)/R_P$, enables the I–V curve

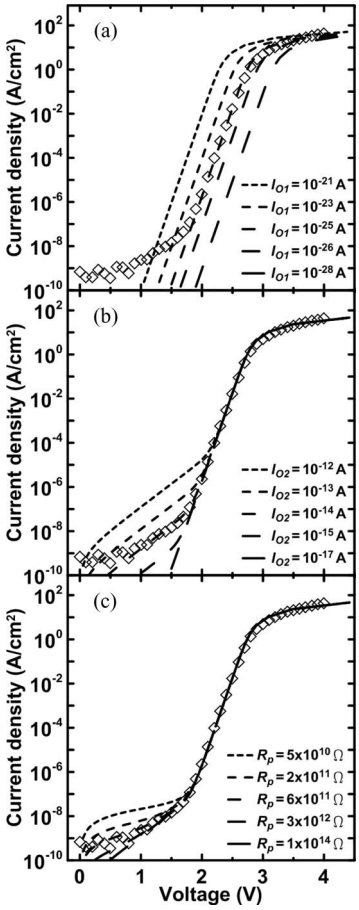

Fig. 3. J–V curve of the conventional InGaN LED on semi-log scale and theoretically fitted using (4) with adjusted variables (a) I_{O1}, (b) I_{O2}, and (c) R_P.

of an InGaN LED to be rewritten as

$$I = A \cdot J = I_{O1}\left(\exp\left(\frac{e(V - IR_S)}{n_1 kT}\right) - 1\right) + I_{O2}\left(\exp\left(\frac{e(V - IR_S)}{n_2 kT}\right) - 1\right) + \frac{(V - IR_S)}{R_P} \quad (4)$$

where A and J denote the mesa area and the injected current density of the LED, respectively.

Fig. 3 plots the J–V curve of the conventional InGaN LED on a semilog scale and theoretically fits it using (4) with variables I_{O1} [Fig. 3(a)], I_{O2} [Fig. 3(b)], and R_P [Fig. 3(c)]. Clearly, adjusting the three parameters I_{O1}, I_{O2}, and R_p enables the experimental J–V curve of the conventional InGaN LED to be well fitted. In Fig. 3, $n_1 = 1.9$, $n_2 = 8$, and $R_S = 21\ \Omega$, obtained experimentally from Fig. 2(a), are used. Notably, according to Fig. 3(b), the diffusion–recombination process becomes less important as I_{O2} increases, indicating that although a relatively large ideality factor of $n_2 = 8$ accompanies the defect-assisted leakage process, as long as the density of dislocation defects is large enough, then most of the injected carriers will recombine promptly at the deep-level traps that are associated with the dislocation defects, without any diffusion–recombination process. Restated, the saturation current is an important index of the dominant of the recombination of injected carriers in an InGaN LED. Moreover, as displayed in Fig. 3(c), in the region to which a small forward bias (<1 V) is applied, the parallel resistance (R_P) dominates the leakage current. The calculated saturation currents associated with the diffusion–recombination and the defect-assisted leakage processes are $I_{O1} = 1 \times 10^{-25}$ A and $I_{O2} = 1 \times 10^{-14}$ A, respectively. The estimated parallel resistance of the conventional InGaN LED is $R_P = 6 \times 10^{11}\ \Omega$.

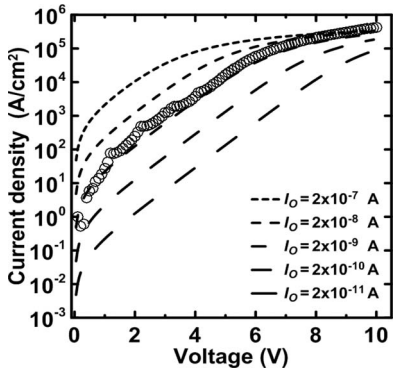

Fig. 4. J–V curve of InGaN nanorod LED on semilog scale, theoretically fit using $n_{\text{ideal}} = 25$ and $R_S = 22\ \text{k}\Omega$.

Similarly, Fig. 4 plots the J–V curve of the nanorod LED in a semilog scale. Clearly, one major recombination process of injected carriers dominates the J–V curve of the nanorod LED. No diffusion–recombination current ($1.0 < n_{\text{ideal}} < 2.0$) is observed in Fig. 4, since the rectification behavior of the nanorod LED exhibits an extremely large ideality factor of $n_{\text{ideal}} = 25$. Again, the experimental J–V curve was fitted using (4), and therefore, the diffusion—recombination of injected carriers was neglected. In addition, the experimental J–V curve can be fitted directly without taking R_P into account, revealing that no injected carriers are leaked or bypass the junction region in the nanorod LED, which will be illustrated more clearly later in the paper. The calculated saturation current of the nanorod LED is $I_O = 2 \times 10^{-9}$ A, determined using $n_{\text{ideal}} = 25$ and $R_S = 22\ \text{k}\Omega$, and is five orders of magnitude larger than $I_{O2} = 1 \times 10^{-14}$ A. This result is consistent with our earlier finding that the defect-assisted leakage current did not dominate in the nanorod LED, and that other recombination processes of injected carriers must occur in the nanorod LED.

To further examine the issue of leakage current of our LED samples, Fig. 5 plots the J–V curve on a semi-log scale from -10 to 2 V for (a) conventional and (b) single nanorod LEDs, respectively. In Fig. 5(a), the J–V curve of the conventional LED can be clearly divided into three regions: region I for the applied bias-voltage less than -5.8 V, region *II* for the applied bias-voltage between -5.8 and 1 V, and region *III* for the applied bias-voltage larger than 1 V. In region I, the measured reverse current density increases exponentially with the increasing of the reverse voltage, entirely due to the breakdown of the conventional LED. The breakdown voltage of the conventional LED (marked by an arrow) is around -5.8 V. In region *II*, the J–V curve is primarily dominated by R_P of the conventional LED and can be well explained by the Ohmic law ($V = I \bullet R_P$, red

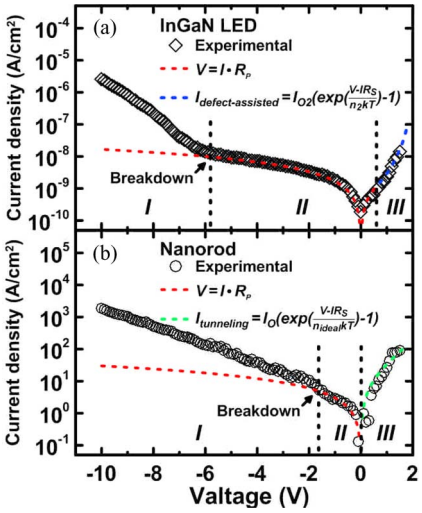

Fig. 5. J–V curves on a semilog scale from -10 to 2 V for (a) conventional and (b) single nanorod LEDs.

dashed-line). Notably, the measured J–V curve of the conventional LED is symmetrical for the applied bias-voltage from -1 to 1 V, indicating R_P still dominates the injected carriers as a small forward bias is applied ($<$1 V). Restated, R_P is mainly caused by the damage of junction regions and by the surface recombination associated with crystalline imperfection. The calculated R_P and measured leakage current at -5 V of the conventional LED are $6 \times 10^{11}\ \Omega$ and 1×10^{-8} A/cm^2, respectively. Finally, in region *III* ($>$1 V), the carrier recombination via trap levels associated with dislocation defects begins in the LED's depletion region and becomes dominated (blue dashed-line), resulting in the ideality factor of $n_{\rm ideal} = 8$, as previously discussed in reference to Fig. 2(a).

Similarly, as shown in Fig. 5(b), the measured J–V curve of the nanorod LED can also be divided into three regions. Accordingly, the measured reverse current density increases rapidly as the reverse voltage increases in region I (<-1.7 V). Again, it is because of the breakdown of the nanorod LED. The breakdown voltage of the nanorod LED (marked by an arrow) is around -1.7 V. In addition, as compared to that of the conventional LED, the smaller gradient of the J–V curve of the nanorod LED in region I is mainly attributed to its inherently small value of R_P. For the applied bias-voltage between -1.7 and 0 V (region *II*), the J–V curve of the nanorod LED is dominated by its R_P. The calculated R_P of the nanorod LED in region *II* is around $1 \times 10^9\ \Omega$. As compared to the conventional LED, the surface recombination events in the nanorod LED with large surface-to-volume ratio will in principle lead to a large leakage current, resulting in a much smaller R_P. Furthermore, such a small R_P of the nanorod LED also affects its J–V curve in region I, as one can observe that the breakdown behavior of the nanorod LED looks analogous to the calculated $V = I \bullet R_P$ curve (red dashed-line). In region *III* ($>$0 V), the J–V curve of the nanorod LED is not symmetrical to which a reverse bias is applied, implying R_P has no influence on the injected carriers in this region. In contrast, the measured forward current increases exponentially with the increasing of the forward voltage and can be described well by $I_{\rm tunneling} = I_o(\exp((e(V - IR_S))/n_{\rm ideal}kT) - 1)$ (green dashed-line), as previously discussed in reference to Fig. 4. Importantly, it indicates the injected carriers are indeed flowing through the junction region of the nanorod LED, even when only a small forward voltage is supplied. We believe the aforementioned observation is mainly attributed to a significant enhancement of tunneling effect on the injected carriers in the nanorod LED. The tunneling effect, enhanced by the nanoscale features of the nanorod LED, induces the transport of injected carriers through the junction region of the nanorod LED. Moreover, for the nanorod LED, this tunneling of injected carriers is extensive as no parasitic effect or diffusion–recombination process is observed under the measuring conditions. Consequently, the saturated current of the nanorod LED is specifying degree of significance enhanced, leading to an unusually and extremely large ideality factor of $n_{\rm ideal} = 25$.

IV. Conclusion

In conclusion, this study elucidates the I–V characteristics of InGaN single nanorod LEDs. Based on a comparison of the conventional InGaN LED with a chip size of $300 \times 300\ \mu$m^2 and the Shockley equation modified to consider the diffusion–recombination and defect-assisted leakage currents as well as the parasitic effect, this study determines that the effect of enhanced tunneling on the injected carriers is mainly responsible for the experimentally observed large saturated current in the InGaN nanorod LED. Results of this study concerning the electrical property of the nanorod LED significantly contribute to the efforts to manufacture nanoscale photonic and optoelectronic devices.

Acknowledgment

The authors gratefully acknowledge technical support from Zyvex Instruments.

References

[1] X. Duan, Y. Huang, Y. Cui, J. Wang, and C. M. Lieber, "Indium phosphide nanowires as building blocks for nanoscale electronic and optoelectronic devices," *Nature*, vol. 409, pp. 66–69, 2001.

[2] W. Lu and C. M. Lieber, "Semiconductor nanowires," *J. Phys. D: Appl. Phys.*, vol. 39, pp. R387–R406, 2006.

[3] W. I. Park, G. C. Yi, M. Kim, and S. J. Pennycook, "Quantum confinement observed in ZnO/ZnMgO nanorod heterostructures," *Adv. Mater.*, vol. 15, pp. 526–529, 2004.

[4] Y. R. Wu, C. H. Chiu, C. Y. Chang, P. Yu, and H. C. Kuo, "Size-dependent strain relaxation and optical characteristics of InGaN/GaN nanorod LEDs," *IEEE J. Sel. Top. Quantum Electron.*, vol. 15, no. 4, pp. 1226–1233, Jul./Aug. 2009.

[5] H. M. Kim, D. S. Kim, D. Y. Kim, T. W. Kang, Y. H. Cho, and K. S. Chung, "Growth and characterization of single-crystal GaN nanorods by hydride vapor phase epitaxy," *Appl. Phys. Lett.*, vol. 81, pp. 2193–2195, 2002.

[6] J. C. Johnson, H.-J. Choi, K. P. Knutsen, R. D. Schaller, P. Yang, and R. J. Saykally, "Single gallium nitride nanowire lasers," *Nat. Mater.*, vol. 1, pp. 106–110, 2002.

[7] M. H. Huang, S. Mao, H. Feick, H. Yan, Y. Wu, H. Kind, E. Weber, R. Russo, and P. Yang, "Room-temperature ultraviolet nanowire nanolasers," *Science*, vol. 292, pp. 1897–1899, 2001.

[8] H.-M. Kim, Y. H. Cho, H. Lee, S. I. Kim, S. R. Ryu, D. Y. Kim, T. W. Kang, and K. S. Chung, "High-brightness light emitting diodes using

dislocation-free indium gallium nitride/gallium nitride multiquantum-well nanorod arrays," *Nano Lett.*, vol. 4, pp. 1059–1062, 2004.

[9] L. Y. Chen, Y. Y. Huang, C. H. Chang, Y. H. Sun, Y. W. Cheng, M. Y. Ke, C. P. Chen, and J. J. Huang, "High performance InGaN/GaN nanorod light emitting diode arrays fabricated by nanosphere lithography and chemical mechanical polishing processes," *Opt. Exp.*, vol. 18, pp. 7664–7669, 2010.

[10] C. H. Chiu, T. C. Lu, H. W. Huang, C. F. Lai, C. C. Kao, J. T. Chu, C. C. Yu, H. C. Kuo, S. C. Wang, C. F. Lin, and T. H. Hsueh, "Fabrication of InGaN/GaN nanorod light-emitting diodes with self-assembled Ni metal islands," *Nanotechnology*, vol. 18, pp. 445201-1–445201-4, 2007.

[11] H. W. Huang, C. C. Kao, T. H. Hsueh, C. C. Yu, C. F. Lin, J. T. Chu, H. C. Kuo, and S. C. Wang, "Fabrication of GaN-based nanorod light emitting diodes using self-assemble nickel nano-mask and inductively coupled plasma reactive ion etching," *Mater. Sci. Eng. B*, vol. 113, pp. 125–129, 2004.

[12] D. Zhu, J. Xu, A. N. Noemaun, J. K. Kim, E. F. Schubert, M. H. Crawford, and D. D. Koleske, "The origin of the high diode-ideality factors in GaInN/GaN multiple quantum well light-emitting diodes," *Appl. Phys. Lett.*, vol. 94, pp. 081113-1–081113-3, 2009.

[13] X. A. Cao, J. M. Teetsov, M. P. D'Evelyn, D. W. Merfeld, and C. H. Yan, "Electrical characteristics of InGaNGaN light-emitting diodes grown on GaN and sapphire substrates," *Appl. Phys. Lett.*, vol. 85, pp. 7–9, 2004.

[14] S. W. Lee, D. C. Oh, H. Goto, J. S. Ha, H. J. Lee, T. Hanada, M. W. Cho, T. Yao, S. K. Hong, H. Y. Lee, S. R. Cho, J. W. Choi, J. H. Choi, J. H. Jang, J. E. Shin, and J. S. Lee, "Origin of forward leakage current in GaN-based light-emitting devices," *Appl. Phys. Lett.*, vol. 89, pp. 132117-1–132117-3, 2006.

Ya-Ju Lee received the B.S. degree in physics from the National Central University, Jhongli, Taiwan, in 2000 and the M.S. and Ph.D. degrees from the National Chiao Tung University, Hsinchu, Taiwan, in 2002 and 2007, respectively.

In 2008, he was a Postdoctoral Research Associate in the Future Chips Constellation and Department of Physics, Applied Physics and Astronomy, Rensselaer Polytechnic Institute, Troy, NY. Since February 2009, he has been with the National Taiwan Normal University, Taipei, Taiwan, as a Faculty Member of the Institute of Electro-Optical Science and Technology. His current research interests include the theoretical and experimental aspects of the physics of semiconductor optoelectronics materials and devices.

Chia-Jung Lee received the B.S. degree from the Minghsin University of Science and Technology, Hsinchu, Taiwan, in 2008. He is currently working toward the Master's degree in the Institute of Electro-Optical Science and Technology, National Taiwan Normal University, Taipei, Taiwan.

His current research interest includes high-performance III–V semiconductor LEDs.

Chih-Hao Chen received the B.S. degree in materials science from the National University of Tainan, Tainan, Taiwan, in 2008 and the M.S. degree from the Institute of Electro-Optical Science and Technology, National Taiwan Normal University, Taipei, Taiwan, in 2010.

He is currently with the Institute of Electro-Optical Science and Technology, National Taiwan Normal University, Taipei, Taiwan.

Tien-Chang Lu (M'07) received the B.S. degree in electrical engineering from the National Taiwan University, Taipei, Taiwan, in 1995, the M.S. degree in electrical engineering from the University of Southern California, Los Angeles, in 1998, and the Ph.D. degree in electrical engineering and computer science from the National Chiao Tung University, Hsinchu, Taiwan, in 2004.

In 2004, he was with the Union Optronics Corporation as a Manager of the Epitaxy Department. Since August 2005, he has been with the National Chiao Tung University as a Member of the Faculty in the Department of Photonics. He is involved in the low-pressure metal–organic chemical vapor deposition (MOCVD) epitaxial technique associated with various material systems as well as the corresponding process skills. His current research interests include the design, epitaxial growth, process, and characterization of optoelectronic devices, structure design and simulations for optoelectronic devices using computer-aided software. He is the author and coauthor of more than 150 internal journal papers.

Dr. Lu was the recipient of The Exploration Research Award of the Pan Wen Yuan Foundation in 2007 and Excellent Young Electronic Engineer Award in 2008.

Hao-Chung Kuo (M'98–SM'06) received the B.S. degree in physics from the National Taiwan University, Taipei, Taiwan, the M.S. degree in electrical and computer engineering from Rutgers University, New Brunswick, NJ, in 1995, and the Ph.D. degree from the University of Illinois at Urbana Champaign, Champaign, IL, in 1999.

He has an extensive professional career both in research and industrial research institutions that includes: Research Consultant in Lucent Technologies, Bell Laboratories during 1993–1995; a Member of Technical Staff in Fiber-Optics Division at Agilent Technologies during 1999–2001, and LuxNet Corporation during 2001–2002. Since October 2002, he has been with the National Chiao Tung University (NCTU), Hsinchu, Taiwan, as a Faculty Member of the Institute of Electro-Optical Engineering. He is now the Associate Dean, Office of International Affair, NCTU. His current research interests include semiconductor lasers, vertical-cavity surface-emitting lasers, blue and ultraviolet LED lasers, quantum-confined optoelectronic structures, optoelectronic materials, and solar cells. He is the author and coauthor of 140 internal journal papers and six granted and ten pending patents.

Dr. Kuo is an Associate Editor of the IEEE/OSA JOURNAL OF LIGHTWAVE TECHNOLOGY and the IEEE JOURNAL OF SELECTED TOPICS IN QUANTUM ELECTRONICS-special issue Solid State Lighting. He was the recipient of Ta-You Wu Young Scholar Award from National Science Council and Young Photonics Researcher Award in 2007.